JOURNAL OF APPLIED ELECTROCHEMISTRY **27** (1997) 1307–1309

SHORT COMMUNICATION

Effect of Br^- on electrochemical performance of the hydrogen storage alloy $MlNi_{3.45}(CoMnTi)_{1.55}$ electrode

S. A. CHENG*, Y. Q. LEI‡, H. LIU*, Q. D. WANG‡, J. Q. ZHANG*, C. N. CAO*

Department of Chemistry and Department of Materials Science and Engineering‡, Zhejiang University, Hangzhou, 310027, People's Republic of China*

Received 2 January 1997; revised 10 April 1997

1. Introduction

Nickel–metal hydride (Ni/MH) batteries using hydrogen storage alloys as negative electrodes constitute a new kind of high energy density batteries. Compared with the Ni/Cd rechargeable batteries they have many merits such as high capacity, long-life rechargeable, no memory effect, faster charging–discharging rate, as well as their being pollution free [1–5]. Three types of storage alloy, namely AB_5, AB/A_2B and AB_2, have been adopted in recent years [6–9], but the cycle life of the alloys all decrease on cycling due to surface cracking and oxidization [10]. Surface treatment is found to be an effective way of prolonging cycle life. The main surface treatments are: (i) pretreatment of the alloy powder in an acid, alkaline or salt solution [11], and (ii) microencapsulation of the alloy by electroless coating of copper or nickel [12]. Encapsulated layers are effective in improving the performance of negative electrodes by reducing poisoning of the alloy and by improving its electrical conductivity. But alloy pulverization on cycling may partly destroy the protective layer and reduce the cycle life of the electrode. The authors believe that it would be effective if the protective layer can be restored during the period of charging–discharging. In the present investigation the electrochemical performances of the hydrogen storage alloy $MlNi_{3.45}(CoMnTi)_{1.55}$ (Ml–lanthanum rich misch metal) electrode in 6 M KOH containing KBr were studied. The results were promising and may lead to new ways of protecting hydrogen storage alloy electrodes from oxidation.

2. Experimental details

The hydrogen storage alloy $MlNi_{3.45}(CoMnTi)_{1.55}$ was prepared by vacuum induction melting and pulverized to 20–63 μm particle size by repeated hydrogen absorption–desorption cycling. The test electrodes were fabricated by filling the alloy particles into porous nickel substrates (size: 15 mm × 15 mm× 0.8 mm), employing 3 wt % polyvinyl alcohol (PVA) as a binder and then pressing to a thickness of 0.5 mm after drying at 50 °C in air for 5 h.

The electrochemical capacity of the negative electrode was measured using a Pyrex glass cell in which three compartments were separated from each other by sintered glass filters. The counter electrode was a $Ni(OH)_2$ positive electrode with much larger capacity and a mercury oxide electrode (Hg/HgO, 6 M KOH) was used as reference. The electrolyte was 6 M KOH solution containing potassium bromide. Potassium bromide in concentrations of 0.0, 0.1, 0.5, 1.0 and 2.0 M was added. The negative electrode was cycled first ten times with charging for 7 h and discharging to 0.6 V vs Hg/HgO both at 60 mA g^{-1} to obtain the maximum electrochemical capacity of the alloy, C_{60}. The capacities of the negative electrode at various discharge currents, C_R were then measured. The discharge rate capability of the electrode was evaluated using the equation:

$$\gamma = \frac{C_R}{C_{60}} \times 100\% \qquad (1)$$

where γ is the discharge rate capability, C_R is the discharge capacity of the electrode at the current R (mA g^{-1}) and C_{60} is the discharge capacity of the electrode at 60 mA g^{-1} current.

To avoid loss of alloy powder during charge–discharge cycling, the negative electrode was placed between two NiOOH– $Ni(OH)_2$ counter electrodes separated by Nylon cloth, clamped from the outside using two porous acrylic resin sheets. Cycling tests were performed by charging at 300 mA g^{-1} for 1.2 h and discharging at 300 mA g^{-1} to −600 mV vs Hg/HgO. After measurements, the electrode was charged again for 3 h at 60 mA g^{-1} before the cyclic voltammetry in the potential range from −1.0 to 0 V vs Hg/HgO with sweep rate 30 mV s^{-1}.

Surface morphology and composition were characterized by scanning electron microscopy (SEM) and X-ray photoelectron spectroscopy (XPS), respectively.

3. Results and discussion

The effect of Br^- concentration on the discharge capacity of the negative electrode is shown in Fig. 1. In the electrolyte without KBr the saturation capacity of electrode is reached at the sixth cycle, while the saturation capacity in electrolyte containing KBr is reached at the second cycle. The saturation capacity increases with increasing KBr concentration. The maximum is at 1 M KBr from the standpoint of practical application. This indicates that Br^- improves the surface state of the electrode. The relationship between the capacity and the cycle number is

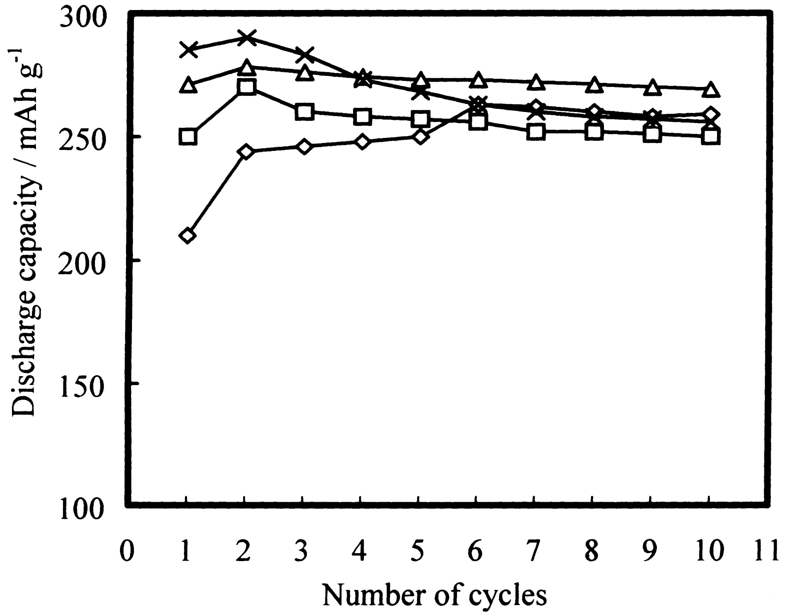

Fig. 1. Discharge capacity of the electrode in the electrolyte: (◇) without KBr, (□) with 0.5 M KBr, (Δ) with 1.0 M KBr, (×) with 2.0 M KBr as a function of cycle number at 25 °C.

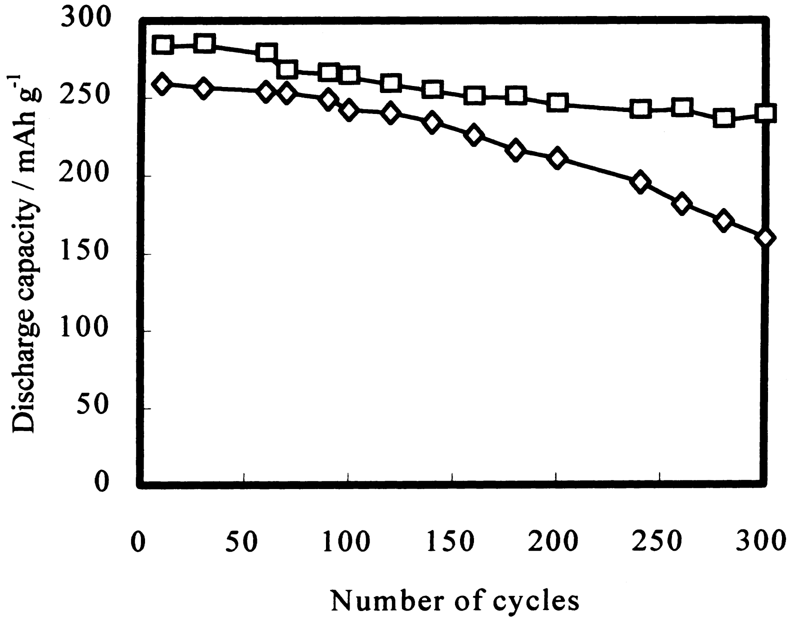

Fig. 2. Charge/discharge cycle characteristics of the electrode in the electrolyte: (◇) without KBr, (□) with 1.0 M KBr at at 25 °C.

shown in Fig. 2. The cycle life of the cell containing KBr is obviously higher than that of the cell without KBr. After 300 cycles the capacity of the electrode in electrolyte with KBr decays only 14%, while the capacity decay of the electrode in electrolyte without KBr is 28%. The SEM micrographs, shown in Figs 3 and 4, indicate that there are many corrosion products on the alloy surface in electrolyte without KBr and the profile of alloy particles is clean and there are many fine bromide needles on the alloy surface for electrolyte with added KBr. The XPS results indicate that in electrolyte without KBr the La and Ni on the alloy surface are in the form of oxide and hydroxide and in electrolyte with KBr rare earth bromides exist in the surface layer. The bromide protects the alloy

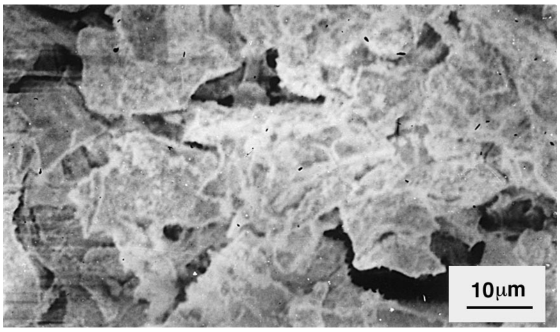

Fig. 3. SEM micrograph of the cycled electrode surface in the electrolyte without KBr.

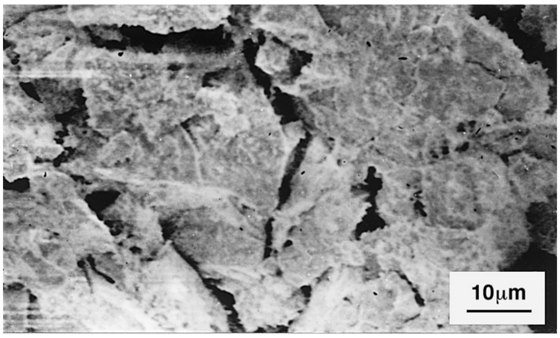

Fig. 4. SEM micrograph of the cycled electrode surface in the electrolyte with KBr.

surface from oxidation and, at the same time, catalyses the hydrogen absorption–desorption process. The reaction process is believed to be as follows:

$$\mathrm{Br^- + M \Leftrightarrow MBr^-_{abs}} \tag{2}$$

$$\mathrm{MBr^-_{abs} + H_2O \Leftrightarrow MBr^-_{abs} \ldots H + OH^- + e^-} \tag{3}$$

$$\mathrm{MBr^-_{abs} \ldots H + M \Leftrightarrow MH + Br^-} \tag{4}$$

where M and MH are the hydrogen storage alloy and its hydride respectively, $\mathrm{MBr^-_{abs}}$ the active complex between $\mathrm{Br^-}$ and surface of the alloy, $\mathrm{MBr^-_{abs} \ldots H}$ a hydrogen atom adsorbed on the active complex.

A cyclic voltammogram of the electrode in the potential range of −1.0 to 0 V is shown in Fig. 5. The anodic peak intensity of the electrode in electrolyte containing and not containing KBr appears at −0.64 and −0.66 V vs Hg/HgO, respectively. $\mathrm{Br^-}$ addition produces an increase in anodic peak intensity and a movement of peak position in the negative direction. The cathodic peak does not appear in the investigated potential range due to the very fast hydrogen absorption. This indicates that adding $\mathrm{Br^-}$ promotes hydrogen absorption and desorption at the electrode. Figure 6 shows that the discharge rate capability of the modified electrode increases markedly.

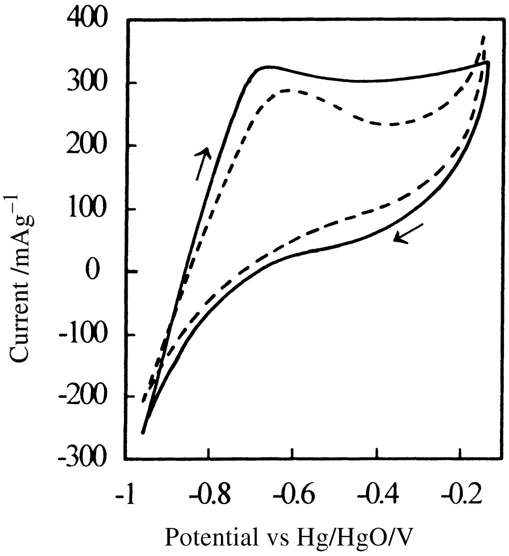

Fig. 5. Cyclic voltammograms of the electrode in the electrolyte: (——) with KBr and (– – –) without KBr at 25 °C.

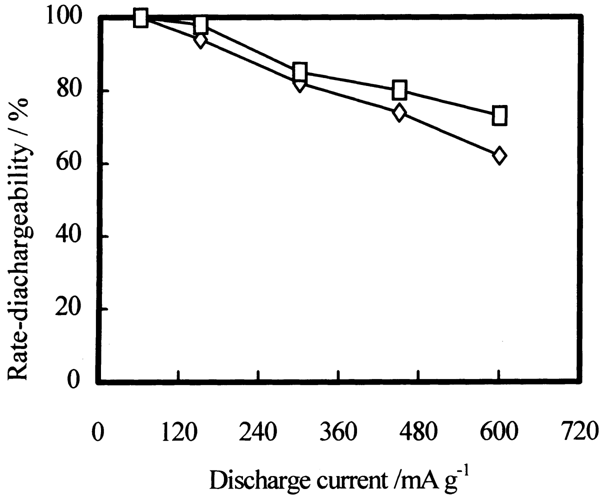

Fig. 6. Discharge rate capability of $\mathrm{MlN_{3.45}(CoMnTi)_{1.55}}$ electrode in the electrolyte: (◇) without KBr, (□) with 1.0 M KBr as a function of discharge current at 25 °C .

4. Conclusion

(i) $\mathrm{Br^-}$ addition promotes the hydrogen absorption and desorption of the hydrogen storage alloy electrode. The capacity and the discharge rate capability of the electrode are all increased.

(ii) The cycle life of the electrode is increased due to the presence of rare earth bromide on the surface of hydrogen storage alloy, which protects the electrode surface from oxidation.

Acknowledgements

The author thanks the Zhejiang Provincial Natural Science Foundation of China for support of this work.

References

[1] Y. Q. Lei, Z. P. Li, C. P. Chen, J. Wu and Q. D. Wang, *J. Less-Common Met*. **172–174** (1991) 1265–1272.

[2] T. Sakai, H. Yoshinaga, H. Miyamura, N. Kuriyama and H. Ishikowa, *J. Alloys Comp*. **180** (1992) 32–35.

[3] C. N. Park and R. Kirchheim, *ibid*. **182** (1992) 321–330.

[4] J. J. G. Williems, *Philips J. Res*. **39** (1984) 1.

[5] J. J. G. Wiliems and K. H. J. Buschow, *J. Less-Common Met*. **129** (1987) 13.

[6] H. F. Bittner and C. C. Badcock, *J. Electrochem. Sor*. **130** (1983) 193.

[7] T. Sakai, H. Miyamura, N. Kuriyama, H. Ishikawa and I. Vehare, *J. Alloys Comp*. **192** (1993) 155–157.

[8] Y. Moriwaki, T. Gamo, H. Seri, T. Iwaki, *J. Less-Common Met*. **172–174** (1991) 1211.

[9] S. Wakao, H. Sawa and J. Furukawa, *ibid*. **172–174** (1991) 1219.

[10] L. Schlapbach, A. Seiler, F. Stucki and H. C. Siegmann, *ibid*. **73** (1980) 145–160.

[11] K. Ikawa, T. Horiba, T. Ogura and Y. Nomura, *Denki Kagaku* **62** (1994) 822–829.

[12] M. Matsuoka, K. Asai, K. Asai, Y. Fukumoto and C. Iwakura, *J. Alloys Comp*. **192** (1993) 149–151.